Diffractive Dijet Production with a Leading Proton in ep Collisions at HERA

Abstract

The cross section of diffractive process $e^+p \to e^+Xp$ is measured at centre-of-mass energies of 320 GeV, where the system X contains at least two jets and the leading final state proton p is detected in the H1 Very Forward Proton Spectrometer (VFPS). The measurement is performed for photoproduction with photon virtualities $Q^2 < 2\,\mathrm{GeV}^2$ and for deep-inelastic-scattering with $4\,\mathrm{GeV}^2 < Q^2 < 80\,\mathrm{GeV}^2$ (for complete phase spaces definiton see Tab. 1). The results are compared to next-to-leading order QCD calculations based on diffractive parton distribution functions as extracted from measurements of inclusive cross sections in diffractive deep-inelastic-scattering. A collinear QCD factorisation prediction is tested against the measured cross sections and their ratios.

PHP	DIS
$Q^2 < 2\,\mathrm{GeV}^2$	$4\,\mathrm{GeV}^2 < Q^2 < 80\,\mathrm{GeV}^2$
Common Cuts	
$0.2 < y < 0.7$	
$E_T^{*\mathrm{jet1}} > 5.5\,\mathrm{GeV}$	$E_T^{*\mathrm{jet2}} > 4.0\,\mathrm{GeV}$
$-1 < \eta^{\mathrm{jet1}} < 2.5$	$-1 < \eta^{\mathrm{jet2}} < 2.5$
$|t| < 0.6\,\mathrm{GeV}^2$	$0.010 < x_{I\!P} < 0.024$
$z_{I\!P} < 0.8$	

Tab. 1: Phase space of the diffractive dijet VFPS measurement (PHP and DIS)

The cross section double ratio of data to NLO prediction for photoproduction and DIS is established as:

$$\frac{(\mathrm{DATA/NLO})_{\gamma p}}{(\mathrm{DATA/NLO})_{\mathrm{DIS}}} = 0.55 \pm 0.10\,(\mathrm{data}) \pm 0.02\,(\mathrm{theor.}) \tag{1}$$

1

	PHP	DIS
Data	$242 \pm 15\,\text{(stat.)} \pm 33\,\text{(syst.)}\,\text{pb}$	$29.7 \pm 2.0\,\text{(stat.)} \pm 2.7\,\text{(syst.)}\,\text{pb}$
NLO QCD	$400^{+140}_{-90}\,\text{(scale)} \pm 80\,\text{(DPDF)}\,\text{pb}$	$27.2^{+10.2}_{-5.9}\,\text{(scale)} \pm 5.3\,\text{(DPDF)}\,\text{pb}$
Data/NLO	$0.60 \pm 0.08\,\text{(data)} \pm 0.21\,\text{(theor.)}$	$1.09 \pm 0.10\,\text{(data)} \pm 0.40\,\text{(theor.)}$

Tab. 2: The integrated diffractive cross section of dijet production for photoproduction (PHP) and deep-inelastic-scattering (DIS) compared to NLO QCD calculations with H1 2006 Fit B DPDFs. The data cross sections are complemented by statistical and systematical uncertainties. For the theoretical predictions the uncertainties from NLO scale variation and H1 Fit B DPDFs are presented. The suppression ratios in the last row are supplemented by the experimental and theoretical uncertainties.
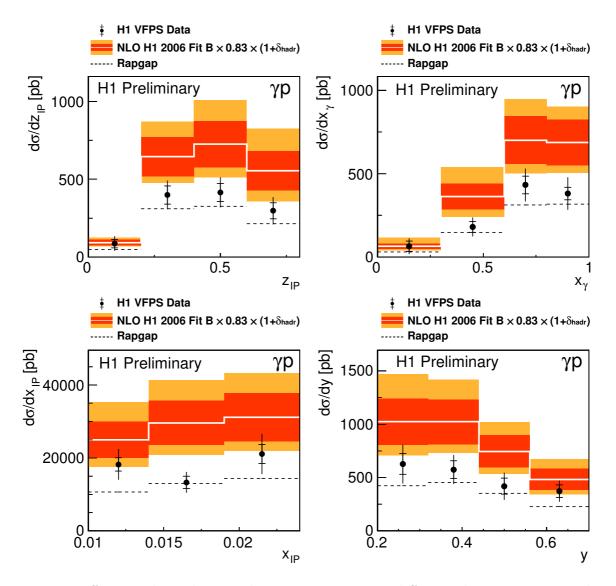
Fig. 1: Diffractive dijet photoproduction cross sections differential in $z_{I\!\!P}$, x_γ, $x_{I\!\!P}$ and y. The inner error bars represent the statistical errors. The outer error bars indicate the statistical and systematic errors added in quadrature. NLO QCD predictions based on the DPDF set H1 2006 Fit B and GRV HO γ-PDF, corrected to the level of stable hadrons, are shown as a white line. The red bands indicate the DPDFs uncertainties and the orange bands indicate the DPDFs and scale uncertainties of the theoretical calculations added in quadrature.
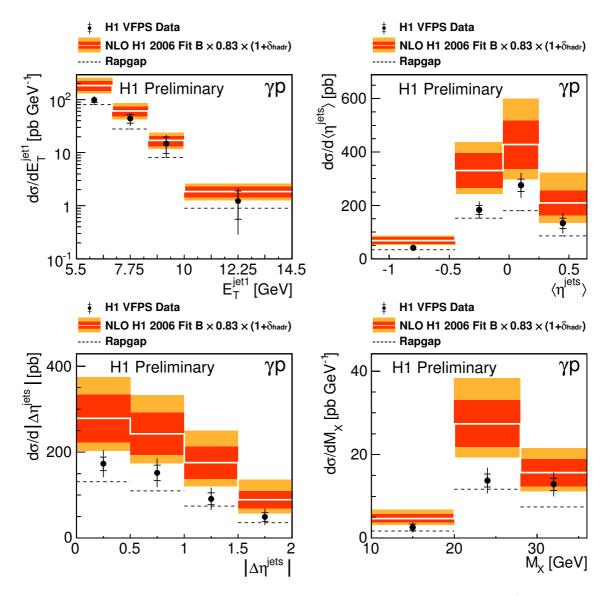
3

Fig. 2: Diffractive dijet photoproduction cross sections differential in E_T^{jet1}, $\langle \eta^{\text{jets}} \rangle$, $|\Delta\eta^{\text{jets}}|$ and M_X. The inner error bars represent the statistical errors. The outer error bars indicate the statistical and systematic errors added in quadrature. NLO QCD predictions based on the DPDF set H1 2006 Fit B and GRV HO γ-PDF, corrected to the level of stable hadrons, are shown as a white line. The red bands indicate the DPDFs uncertainties and the orange bands indicate the DPDFs and scale uncertainties of the theoretical calculations added in quadrature.
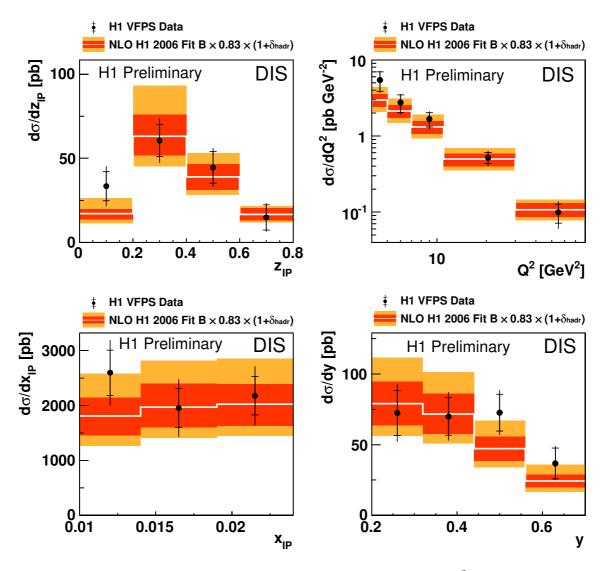
Fig. 3: Diffractive dijet DIS cross sections differential in $z_{I\!P}$, Q^2, $x_{I\!P}$ and y. The inner error bars represent the statistical errors. The outer error bars indicate the statistical and systematic errors added in quadrature. NLO QCD predictions based on the DPDF set H1 2006 Fit B, corrected to the level of stable hadrons, are shown as a white line. The red bands indicate the DPDFs uncertainties and the orange bands indicate the DPDFs and scale uncertainties of the theoretical calculations added in quadrature.
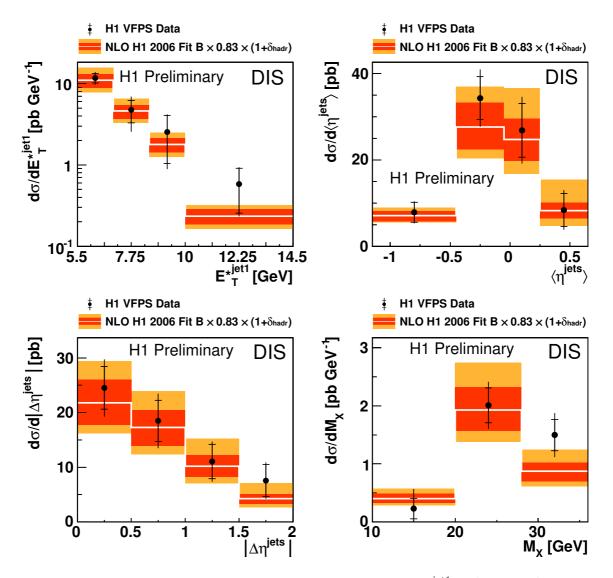
5

Fig. 4: Diffractive dijet DIS cross sections differential in $E_T^{*\text{jet1}}$, $\langle \eta^{\text{jets}} \rangle$, $|\Delta \eta^{\text{jets}}|$ and M_X. The inner error bars represent the statistical errors. The outer error bars indicate the statistical and systematic errors added in quadrature. NLO QCD predictions based on the DPDF set H1 2006 Fit B, corrected to the level of stable hadrons, are shown as a white line. The reds bands indicate the DPDFs uncertainties and the orange bands indicate the DPDFs and scale uncertainties of the theoretical calculations added in quadrature.
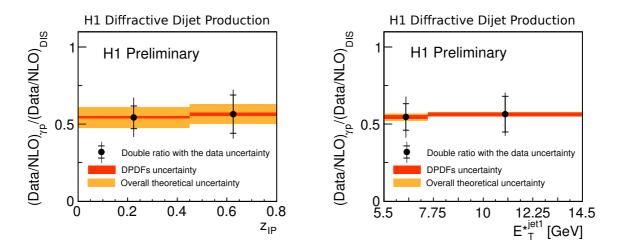
Fig. 5: Cross section double ratios of data to NLO prediction for photoproduction and DIS as a function of the $z_{I\!P}$ and $E_T^{*\mathrm{jet1}}$. The inner error bars represent the data statistical errors, the outer error bars indicate the data statistical and systematic errors added in quadrature. The red bands indicate the DPDFs uncertainties and the orange bands indicate the DPDFs and scale theoretical uncertainties of the double ratios added in quadrature.
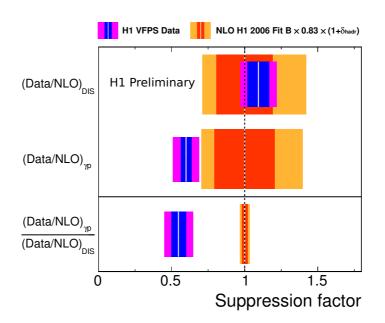
Fig. 6: DIS and photoproduction (γp) integrated cross sections normalised to the NLO theoretical calculations are shown as a white line. The integrated cross section double ratio of data to NLO prediction for photoproduciton and DIS is presented as a white line in the last row. The blue bands indicate the data statistical uncertainties and the violet band indicate the statistical and systematic experimental uncertainties added in quadrature. In addition the DPDFs uncertainties (red bands) and the DPDFs and scale uncertainties added in quadrature (orange bands) are presented.